HHS Public Access

Author manuscript

Neuroimage. Author manuscript; available in PMC 2021 March 12.

Published in final edited form as:

Neuroimage. 2021 March ; 228: 117728. doi:10.1016/j.neuroimage.2021.117728.

PET measurement of longitudinal amyloid load identifies the earliest stages of amyloid-beta accumulation during Alzheimer's disease progression in Down syndrome

Matthew D. Zammit[a,*], **Dana L. Tudorascu**[b], **Charles M. Laymon**[c,d], **Sigan L. Hartley**[a], **Shahid H. Zaman**[e], **Beau M. Ances**[f], **Sterling C. Johnson**[g], **Charles K. Stone**[h], **Chester A. Mathis**[b], **William E. Klunk**[b], **Ann D. Cohen**[b], **Benjamin L. Handen**[b], **Bradley T. Christian**[a]

[a]University of Wisconsin-Madison, Waisman Center, 1500 Highland Avenue, Madison, WI 53705, United States

[b]University of Pittsburgh, Department of Psychiatry, Pittsburgh, PA, United States

[c]University of Pittsburgh, Department of Radiology, Pittsburgh, PA, United States

[d]University of Pittsburgh, Department of Bioengineering, Pittsburgh, PA, United States

[e]Cambridge Intellectual Disability Research Group, University of Cambridge, Cambridge, United Kingdom

[f]Washington University in St. Louis Department of Neurology, St. Louis, MO, United States

[g]University of Wisconsin-Madison, Alzheimer's Disease Research Center, Madison, WI, United States

[h]University of Wisconsin-Madison, Department of Medicine, Madison, WI, United States

[*]Corresponding author. mzammit@wisc.edu (M.D. Zammit).

Author contributions

Matthew D. Zammit: Conceptualization, methodology, writing – original draft
Dana L. Tudorascu: Methodology, writing – review & editing
Charles L. Laymon: Writing – review & editing
Sigan L. Hartley: Writing – review & editing
Shahid H. Zaman: Writing – review & editing
Beau M. Ances: Writing – review & editing
Sterling C. Johnson: Methodology, writing – review & editing
Chales K. Stone: Writing – review & editing
Chester A. Mathis: Writing – review & editing
William E. Klunk: Funding acquisition, writing – review & editing
Ann D. Cohen: Writing – review & editing
Benjamin L. Handen: Funding acquisition, writing – review & editing
Bradley T. Christian: Funding acquisition, supervision, conceptualization, writing – review & editing

Data availability statement

The University of Wisconsin-Madison and University of Pittsburgh sites have entered web-based data through the Alzheimer's Therapeutic Research Institute (ATRI) as part of the ABC-DS study. Data from the ABC-DS study and research methodology is currently available to the scientific community through the LONI database.

Declaration of Competing Interest

GE Healthcare holds a license agreement with the University of Pittsburgh based on the technology described in this manuscript. Dr. Klunk is a co-inventor of PiB and, as such, has a financial interest in this license agreement. GE Healthcare provided no grant support for this study and had no role in the design or interpretation of results or preparation of this manuscript. All other authors have no conflicts of interest with this work and had full access to all of the data in the study, and take responsibility for the integrity of the data and the accuracy of the data analysis.

Abstract

Introduction: Adults with Down syndrome (DS) are predisposed to Alzheimer's disease (AD) and reveal early amyloid beta (Aβ) pathology in the brain. Positron emission tomography (PET) provides an in vivo measure of Aβ throughout the AD continuum. Due to the high prevalence of AD in DS, there is need for longitudinal imaging studies of Aβ to better characterize the natural history of Aβ accumulation, which will aid in the staging of this population for clinical trials aimed at AD treatment and prevention.

Methods: Adults with DS (N = 79; Mean age (SD) = 42.7 (7.28) years) underwent longitudinal [C-11]Pittsburgh compound B (PiB) PET. Global Aβ burden was quantified using the amyloid load metric (Aβ_L). Modeled PiB images were generated from the longitudinal Aβ_L data to visualize which regions are most susceptible to Aβ accumulation in DS. Aβ_L change was evaluated across Aβ(−), Aβ-converter, and Aβ(+) groups to assess longitudinal Aβ trajectories during different stages of AD-pathology progression. Aβ_L change values were used to identify Aβ-accumulators within the Aβ(−) group prior to reaching the Aβ(+) threshold (previously reported as 20 Aβ_L) which would have resulted in an Aβ-converter classification. With knowledge of trajectories of Aβ(−) accumulators, a new cutoff of Aβ(+) was derived to better identify subthreshold Aβ accumulation in DS. Estimated sample sizes necessary to detect a 25% reduction in annual Aβ change with 80% power (alpha 0.01) were determined for different groups of Aβ-status.

Results: Modeled PiB images revealed the striatum, parietal cortex and precuneus as the regions with earliest detected Aβ accumulation in DS. The Aβ(−) group had a mean Aβ_L change of 0.38 (0.58) Aβ_L/year, while the Aβ-converter and Aβ(+) groups had change of 2.26 (0.66) and 3.16 (1.34) Aβ_L/year, respectively. Within the Aβ(−) group, Aβ-accumulators showed no significant difference in Aβ_L change values when compared to Aβ-converter and Aβ(+) groups. An Aβ(+) cutoff for subthreshold Aβ accumulation was derived as 13.3 Aβ_L. The estimated sample size necessary to detect a 25% reduction in Aβ was 79 for Aβ(−) accumulators and 59 for the Aβ-converter/Aβ(+) group in DS.

Conclusion: Longitudinal Aβ_L changes were capable of distinguishing Aβ accumulators from non-accumulators in DS. Longitudinal imaging allowed for identification of subthreshold Aβ accumulation in DS during the earliest stages of AD-pathology progression. Detection of active Aβ deposition evidenced by subthreshold accumulation with longitudinal imaging can identify DS individuals at risk for AD development at an earlier stage.

Keywords

Down syndrome; Amyloid PET; Alzheimer's disease; Longitudinal; Subthreshold amyloid

1. Introduction

Down syndrome (DS) is characterized by triplication of chromosome 21, which results in overexpression of the gene encoding amyloid precursor protein (APP) production and early amyloid-β (Aβ) plaque accumulation (Oyama et al., 1994; Rumble et al., 1989). Aβ plaques are a hallmark of Alzheimer's disease (AD) and adults with DS reveal a sharp increase in AD dementia after age 50 (Schupf, 2002). It is estimated that the lifetime risk of developing

AD in DS is ~ 90% (McCarron et al., 2017, 2014), and the typical survival time following a dementia diagnosis is ~ 4 years (Sinai et al., 2018).

An in vivo measure of Aβ burden can be achieved through positron emission tomography (PET) (Klunk et al., 2004). PET studies in DS have revealed a pattern of early and prominent Aβ retention in the striatum (Handen et al., 2012), which is consistent with the patterns observed in other forms of early-onset AD (e.g., autosomal dominant AD and APP duplication) (Bateman et al., 2012; Klunk et al., 2007; Remes et al., 2008; Villemagne et al., 2009). When evaluating cortical Aβ retention, the patterns observed in DS closely resemble late-onset AD (Annus et al., 2016; Cole et al., 2017; Hartley et al., 2014; Jennings et al., 2015; Landt et al., 2011; Lao et al., 2018, 2016; Mak et al., 2019; Matthews et al., 2016; Rafii et al., 2015, 2017; Sabbagh et al., 2015), with DS showing longitudinal Aβ increases of ~ 3–4%/year (Lao et al., 2017; Tudorascu et al., 2019; Zammit et al., 2020), but with a notable variation in the age of onset and the rate of accumulation.

Longitudinal studies of AD commonly implement PET imaging to evaluate Aβ change, utilizing the standardized uptake value ratio (SUVr) as the PET outcome measure. The SUVr is calculated as the quotient of the PET-measured signal from both a target region and an off-target region, and has been validated as an estimate of the distribution volume ratio (DVR) to provide an index of region of interest Aβ plaque concentration (Lopresti et al., 2005). Longitudinal studies in late-onset AD, such as the Alzheimer's Disease Neuroimaging Initiative, report annual increases of 0.03 SUVr/year (~ 2%/year) when measured with fluorbetapir PET (Whittington and Gunn, 2018). Using PiB PET, the Harvard Aging Brain Study reports that individuals with high PiB retention accumulate Aβ at a rate of 0.03 SUVr/year (~ 2%/year) (Hanseeuw et al., 2019). The Australian Imaging, Biomarkers, and Lifestyle study shows Aβ change of 0.043 PiB SUVr/year (~ 3%/year) in individuals with mild cognitive impairment (MCI) (Villemagne et al., 2013), similar to the rate of change (0.048 PiB SUVr/year) reported in cases of MCI or AD from the Mayo Clinic Study of Aging (Jack et al., 2013).

As a metric, SUVr can be prone to high within-subject variability when assessed longitudinally (Landau et al., 2015; Tryputsen et al., 2015). This variability results in lower statistical power to detect meaningful Aβ accumulation across time (Whittington and Gunn, 2018) and can confound interpretation in longitudinal imaging studies. To reduce the high longitudinal variability and improve upon the sensitivity of SUVr at detecting Aβ change, the PET metric of amyloid load (Aβ_L) was developed as a global (whole brain) outcome measure of Aβ burden. The Aβ_L is calculated by the linear least squares method between the SUVr image and population-derived template images of specific radioligand binding and nonspecific/off-target binding (Whittington et al., 2018; Whittington and Gunn, 2018). When compared against SUVr, Aβ_L improved sensitivity to detect Aβ change due to the suppression of nonspecific binding signal in both late-onset AD populations (Whittington and Gunn, 2018) and in DS (Zammit et al., 2020).

The Alzheimer's Biomarker Consortium – Down Syndrome (ABC-DS) is an ongoing longitudinal study with a large DS cohort aimed at characterizing the progression of AD-related biomarker change (Handen et al., 2020). The objective of the current study was to

characterize longitudinal rates of Aβ accumulation throughout the different stages of the AD continuum in DS. Utilizing the $A\beta_L$ metric, changes in Aβ PET signal at typical subthreshold levels were assessed to characterize the earliest stages of Aβ accumulation in DS. Given the $A\beta_L$ data, modeled PiB SUVr images were generated at the different stages of AD progression to visualize the regional spread of Aβ in DS. Using the longitudinal data from the Aβ(−) accumulators, a new cutoff of Aβ(+) was derived to better identify early subthreshold Aβ change. Finally, estimated sample sizes necessary to detect a 25% reduction in annual Aβ change was determined for DS participants in early and late Aβ accumulation phases.

2. Methods

2.1. Participants

The current sample included 79 adults with DS (mean age (SD) = 42.7 (7.28) years) recruited for an initial project studying the natural history of Aβ deposition in DS by the University of Wisconsin-Madison Waisman Center and the University of Pittsburgh Medical Center, which has since expanded to eight sites and transitioned into the ABC-DS study (Handen et al., 2020). The University of Wisconsin-Madison and University of Pittsburgh sites have entered web-based data through the Alzheimer's Therapeutic Research Institute (ATRI) as part of the ABC-DS study. Data from the ABC-DS study and research methodology is currently available to the scientific community through the LONI database. Consent was obtained during enrollment into the study by the participant or legally designated caregiver. Inclusion criteria included age ≥ 25 years and having a receptive language mental age of at least three years, based upon the Peabody Picture Vocabulary Test Fourth Edition (PPVT) (Dunn and Dunn, 2007). Genetic testing was performed to confirm DS (trisomy 21, mosaicism, or partial translocation). Exclusion criteria included having a prior diagnosis of dementia, an unstable psychiatric condition (e.g. untreated) that impaired cognitive functioning, or a medical condition that was contraindicative of brain imaging scans (e.g. metallic implants).

2.2. Imaging

T1-weighted magnetic resonance imaging (MRI) scans were acquired on a 3T GE Discovery MR750 (Wisconsin) and a Siemens Trio or Prisma (Pittsburgh) for anatomical reference in the analysis. Positron emission tomography (PET) scans were performed on a Siemens ECAT HR + scanner (Wisconsin/Pittsburgh) or a Siemens 4-ring Biograph mCT (Pittsburgh). A target dose of 15 mCi of [C-11]Pittsburgh compound B (PiB) was injected intravenously, and PET scans were used to measure Aβ acquired 50–70 min post-injection (four 5-minute frames). Of the 79 participants, 24 underwent two PiB scans (2.80 (0.49) years apart), while 30 underwent three scans (2.66 (0.84) years apart) and 25 underwent four scans (2.57 (0.66) years apart). In total, 238 PiB scans were acquired for this study. Using the Statistical Parametric Mapping 12 software (SPM12; The Wellcome centre for Human Neuroimaging, UCL Queen Square Institute of Neurology, London, UK), PET frames were re-aligned to correct for motion, averaged, and spatially normalized to the Montreal Neurological Institute 152 space (MNI152) via a DS-specific PET template for PiB as previously described (Lao et al., 2018). For all images, spatial normalization was required to

calculate the amyloid load ($A\beta_L$); a global measure of $A\beta$ burden calculated from the linear least squares method between the PET image and images of specific and nonspecific PiB binding defined in MNI152 space. Standardized uptake value ratio (SUVr) images were generated by voxel normalization to cerebellar gray matter, and the global $A\beta_L$ was calculated following methodology specific to DS PiB images as previously described (Zammit et al., 2020). Using a cutoff of 20 $A\beta_L$, participants were classified as $A\beta(-)$ ($A\beta_L < 20$ for all longitudinal scans), $A\beta$-converter ($A\beta_L < 20$ at baseline and $A\beta_L \geq 20$ at the most recent follow-up visit), or $A\beta(+)$ ($A\beta_L \geq 20$ for all longitudinal scans). No corrections for the partial volume effect were performed, so estimates of longitudinal increase in $A\beta(+)$ individuals with substantial $A\beta_L$ that present atrophy may be conservative. Participant demographics and imaging information are outlined in Table 1.

2.3. Visualization of longitudinal Aβ change

A modeled SUVr image was generated using a participant's $A\beta_L$, nonspecific binding coefficient (ns), and DS population-derived image templates of PiB specific binding (K) and nonspecific binding (NS) as follows (Whittington and Gunn, 2018; Zammit et al., 2020):

$$SUV\,r_i = N\,S_i * ns + K_i * A\beta_L, \quad (1)$$

where i represents the i^{th} voxel of the image. From the longitudinal data, the average baseline $A\beta_L$ and most recent $A\beta_L$ were calculated across all participants in the $A\beta(-)$, $A\beta$-converter and $A\beta(+)$ groups. Additionally, the average nonspecific binding coefficient was calculated. Using these values, Eq. (1) was solved to generate modeled baseline and most recent SUVr images for each group. Difference images were generated by subtracting the baseline SUVr image from the most recent SUVr image and visualized as a 3D surface projection using MANGO (Research Imaging Institute, UT Health Science Center at San Antonio, TX, USA). SUVr change values (SUVr/year) were calculated separately for the anterior cingulate, frontal cortex, parietal cortex, precuneus, striatum and temporal cortex.

2.4. $A\beta_L$ change trajectories

Using the baseline and most recently acquired scan, an $A\beta_L$ change value ($A\beta_L$/year) was calculated for each participant. $A\beta_L$ change was evaluated with respect to age and with respect to global $A\beta_L$ independently using Pearson's partial correlation coefficients while correcting for imaging site. Participant age and $A\beta_L$ change were then independently compared across $A\beta(-)$, $A\beta$-converter, and $A\beta(+)$ groups using analysis of covariance (ANCOVA) while correcting for imaging site. *Post hoc* Student's t-tests were performed for individual group comparisons while adjusting for Bonferroni correction. Models were not adjusted for APOE $\varepsilon 4$ carrier status due to the low percentage of carriers present in the sample and our previous work showing no association between APOE $\varepsilon 4$ status, $A\beta$ and cognition in DS (Hartley et al., 2014; Tudorascu et al., 2019). All statistical analyses were performed using SAS v9.4.

2.5. Identifying subthreshold Aβ accumulation

Longitudinal $A\beta_L$ change values were used to classify subthreshold $A\beta$ accumulators from non-accumulators in the $A\beta(-)$ group using two separate classifiers. First, using a k-means

clustering algorithm with resampling (k = 2 clusters; n = 1000 iterations), a cutoff (C_K) for Aβ accumulation was derived as the midpoint between cluster centers of the Aβ_L change values from all participants. A second cutoff (C_{2SD}) was derived by taking the mean change + 2*SD of the Aβ(−) group. To evaluate the most recent change in Aβ, Aβ_L change values (Aβ_L/year) were calculated from the two most recent PiB scans for each participant. If the Aβ_L change value exceeded the Aβ_L change cutoffs C_K or C_{2SD}, the participant was classified as having an Aβ_L trajectory distinguishable from non-accumulators within the Aβ(−) group. For each cutoff, the Aβ_L change values from the most recent pair of longitudinal scans were compared between the Aβ(−) non-accumulator, Aβ(−) accumulator, Aβ-converter and Aβ(+) groups using ANCOVA while correcting for imaging site. *Post hoc* Student's t-tests were then performed to assess individual group comparisons while adjusting for Bonferroni correction.

A new cutoff of Aβ(+) to better characterize subthreshold Aβ accumulation, indicating the initiation of detectable pathology, given a single PET scan was derived following methodology outlined in Salvadó et al. (2019) to maximize agreement with C_K and C_{2SD} (Salvadó et al., 2019). Briefly, a range of possible Aβ(+) cutoffs (i.e. 10–25 Aβ_L with increments of 0.1 Aβ_L) were compared against C_K and C_{2SD} using the Youden's J Index (YI; sum of the sensitivity and specificity) (Youden, 1950), the overall percentage agreement (OPA; accuracy of true positive and true negative rate), and the area under the curve (AUC) from receiver operating characteristic (ROC) analysis. The YI and OPA response curves were minimally smoothed using the weighted linear least squares method, and the optimal Aβ(+) cutoff was chosen as the value that maximized both YI and OPA.

2.6. Sample size estimations

Estimated sample sizes necessary to detect a 25% reduction in the annual rate of Aβ accumulation were computed, as described elsewhere (Knopman et al., 2020). Briefly, given the Aβ_L change values from the most recent pair of longitudinal scans in DS, groups of Aβ(−) accumulators and Aβ-converter/Aβ(+) individuals were independently assessed to determine the sample sizes needed to detect a 25% reduction in Aβ change with 80% power at alpha 0.01 using two-sample t-test comparisons (two-tailed).

3. Results

3.1. Visualization of longitudinal Aβ change

From the study sample, 36.7% of participants were classified as either an Aβ-converter or Aβ(+). The average time between the baseline and most recent scan for the Aβ(−), Aβ-converter and Aβ(+) groups were 5.01 (2.10), 6.33 (2.31) and 5.18 (1.64) years, respectively. The average baseline Aβ_L in the Aβ(−), Aβ-converter, and Aβ(+) groups were 8.22 (2.32), 11.0 (2.72) and 31.6 (9.06), respectively. The most recent Aβ_L in the Aβ(−), Aβ-converter, and Aβ(+) groups were 10.4 (3.17), 24.9 (3.53) and 48.2 (14.84), respectively. The average nonspecific binding component (ns) was calculated as 1.00 (0.05) for all groups. Given these values and the DS-specific templates of PiB carrying capacity (K) and nonspecific binding (NS), modeled SUVr images were generated to illustrate the spatial patterns of longitudinal Aβ accumulation in DS (Fig. 1). While Aβ_L represents a single global index, it is also

possible to examine changes in specific brain regions with the modeled SUVr images. Regional SUVr difference values (SUVr/year) for each group are displayed in Table 2. Between the baseline and most recent scans, SUVr change from the modeled images was greatest in the striatum (0.060 SUVr/year) for the Aβ-converter group, followed by the precuneus (0.052), parietal cortex (0.047), anterior cingulate (0.043), frontal cortex (0.038) and temporal cortex (0.030). The regional pattern of Aβ accumulation in the Aβ(+) group was similar to the Aβ-converters.

3.2. $A\beta_L$ change trajectories

Between the baseline and most recent scan, the Aβ(−) group displayed a mean $A\beta_L$ change of 0.38 (0.58) $A\beta_L$/year, while the Aβ-converter and Aβ(+) groups displayed a change of 2.26 (0.66) and 3.16 (1.34) $A\beta_L$/year, respectively. Fig. 2 displays the longitudinal $A\beta_L$ trajectories for all participants. A positive association with a large magnitude effect size (Cohen's d) (Cohen, 1992, 1988) was observed between the mean $A\beta_L$ across all available scans for a given participant and the $A\beta_L$ change values (Pearson's R [95% CI] = 0.77 [0.66, 0.85], p<.00001). Aβ groups were distinguishable when evaluated with respect to $A\beta_L$ change (ANCOVA F (df) = 78.5 (2), p < .0001). From the *post hoc* analysis, differences between $A\beta_L$ change for the Aβ(−), Aβ-converter and Aβ(+) groups were statistically significant across all pairings (p < .05 adjusted for Bonferroni correction). Age and $A\beta_L$ change displayed a positive association with a large magnitude effect size (Pearson's R = 0.54 [0.36, 0.68], p < .00001) (Fig. 3). The mean age (SD) of the Aβ(−) group was 39.1 (4.95) years, and the Aβ-converter and Aβ(+) group ages were 46.4 (6.93) and 51.9 (4.04) years, respectively. The Aβ groups significantly differed in age (ANCOVA F (df) = 33.8 (2), p < .0001), with *post hoc* analysis indicating that the Aβ(−) group was significantly younger than the Aβ-converter and Aβ(+) groups, and the Aβ-converter group significantly younger than the Aβ(+) group (p < .05 adjusted for Bonferroni correction). For all associations, imaging site did not influence the model outcomes.

3.3. Identifying subthreshold Aβ accumulation

To identify subthreshold Aβ accumulation, $A\beta_L$ change cutoffs were calculated using the k-means clustering with resampling (C_K) and the mean + 2*SD (C_{2SD}) methods. The cutoffs were defined as C_K = 1.46 $A\beta_L$/year and C_{2SD} = 1.54 $A\beta_L$/year. Using the $A\beta_L$ change values from the two most recent longitudinal time points, 11 (22%) Aβ(−) participants were classified as Aβ(−) accumulators using C_K compared to the 9 (18%) Aβ(−) accumulators using C_{2SD}. Using C_K, Aβ(−) accumulators displayed a mean $A\beta_L$ change value of 2.40 (1.09) $A\beta_L$/year compared to 0.26 (0.62) $A\beta_L$/year for Aβ(−) non-accumulators, while the Aβ-converter and Aβ(+) groups had change values of 3.15 (1.07) and 3.30 (1.46), respectively, when calculated over the two most recent time points (Fig. 4). There was a significant difference in the $A\beta_L$ change values between the Aβ(−) non-accumulator, Aβ(−) accumulator, Aβ-converter and Aβ(+) groups (ANCOVA F (df) = 51.1 (3); p < .0001). *Post hoc* analysis indicated that the $A\beta_L$ change values from the Aβ(−) accumulators were significantly greater than the non-accumulators (p < .05 adjusted for Bonferroni correction), but were not significantly different with the Aβ-converter or Aβ(+) groups. Using C_{2SD}, Aβ(−) accumulators displayed a mean $A\beta_L$ change value of 2.60 (1.11) $A\beta_L$/year compared to 0.32 (0.66) $A\beta_L$/year for Aβ(−) non-accumulators (Fig. 4). $A\beta_L$ change values were

significantly different between the Aβ(−) non-accumulator, Aβ(−) accumulator, Aβ-converter and Aβ(+) groups (ANCOVA F (df) = 50.6 (3); $p < .0001$). From the *post hoc* analysis, the $A\beta_L$ change values from the Aβ(−) accumulators were significantly different from the Aβ(−) non-accumulators ($p < .05$ adjusted for Bonferroni correction), but were not significantly different from the Aβ-converter or Aβ(+) groups. For all associations, imaging site did not influence the model outcomes.

Using the cutoffs C_K and C_{2SD} as reference, a new cutoff of Aβ(+) was derived to better classify subthreshold accumulation given a single PET scan by maximizing the Youden's J Index (YI) and the overall percentage agreement (OPA). With C_K as the reference, the optimal cutoff was determined as 13.0 $A\beta_L$, having YI of 0.77, OPA of 0.89 and an AUC of 0.91. With C_{2SD} as the reference, the optimal cutoff was determined as 13.3 $A\beta_L$, having YI of 0.79, OPA of 0.90 and an AUC of 0.91. YI and OPA response curves for each cutoff are displayed in Fig. 5.

3.4. Sample size estimations

With knowledge of the $A\beta_L$ change values for the Aβ(−) accumulators and Aβ-converter/Aβ(+) individuals, the sample sizes necessary to detect a 25% reduction in annual Aβ accumulation with 80% power at alpha 0.01 (two-tailed) when compared to a hypothetical control group were determined. The estimated sample size per group was 79 for the Aβ(−) accumulators and 59 for the Aβ-converter/Aβ(+) group. The change of 2.40 (1.09) $A\beta_L$/year for the Aβ(−) accumulators and a corresponding 25% reduction was computed translating to a medium effect size (Cohen's d [95% CI]) of 0.55 [0.23, 0.87] difference between groups (i.e. slightly over a half standard deviation difference between the means). Similarly, the change for the Aβ-converter/Aβ(+) group was 3.22 (1.26) $A\beta_L$/year which translates to an effect size of 0.64 [0.27, 1.01] using a 25% reduction. This represents a medium-high effect size of mean differences.

4. Discussion

Due to the high prevalence of AD in DS, it is important to understand the natural history of Aβ accumulation in the DS population to facilitate their inclusion in clinical trials aimed at Aβ plaque clearance, analogous to the Dominantly Inherited Alzheimer's Network – Trials Unit (DIAN-TU) project (Morris et al., 2012) and in preparation for the Trial-Ready Cohort – Down Syndrome (TRC-DS) study (Rafii et al., 2020). Our previous longitudinal research found that nondemented adults with DS evidence faster striatal Aβ accumulation, but slower Aβ accumulation in the frontal cortex and precuneus compared to nondemented elderly without DS who are at risk for late-onset AD, suggesting that early Aβ increases in DS are most prominent in the striatum (Tudorascu et al., 2019). When classifying the DS population into Aβ(−), Aβ-converter, and Aβ(+) groups, rates of striatal Aβ accumulation were also found to be greatest in the Aβ-converters, however, striatal and cortical Aβ accumulation were indistinguishable in the Aβ(+) group (Lao et al., 2017). Together, this previous work suggests that the rate of Aβ accumulation is approximately the same across all brain regions in DS, with the striatum starting the accumulation process earlier than other regions in the preclinical AD phase. The current study builds on these previous findings by showing the

striatum to have the greatest change in the Aβ-converters based on the modeled PiB images. In the Aβ(+) group, the striatum continued to show the greatest SUVr change, and the cortical SUVr change was similar to the striatal rate of change in the Aβ-converters. Our previous work evaluating Aβ_L change in DS revealed longitudinal increases of ~ 3 Aβ_L/year in Aβ(+) individuals (Zammit et al., 2020), which is similar to the rate of increase observed in late-onset AD when measured with Aβ_L (Whittington and Gunn, 2018). In the current study, further classifying participants by Aβ-status revealed that both Aβ(+) individuals and individuals that converted from Aβ(−) to Aβ(+) at the most recent scan showed longitudinal increases of ~ 3 Aβ_L/year, while Aβ(−) individuals on an Aβ-accumulating trajectory showed increase of ~2 Aβ_L/year. In our sample, the typical age of conversion to Aβ(+) when considering global Aβ in DS was ~ 46 years, with the youngest observed case of Aβ-conversion at age 33 years. Since Aβ is uniformly detected in DS much earlier than late-onset AD with similar global rates of longitudinal increase, DS as a population is well suited for inclusion in anti-Aβ clinical trials.

To better characterize the earliest stages of Aβ progression in DS, Aβ_L change was used to distinguish Aβ(−) participants that were evidencing increases in Aβ accumulation compared to those that were not yet accumulating Aβ. To identify Aβ accumulation, two separate classifier methods were performed and compared using the Aβ_L change data. The first cutoff (C_K) was generated by performing k-means clustering with resampling across all change values, and a second, more conservative cutoff (C_{2SD}) was derived by taking the mean + 2*SD of the change from the Aβ(−) group. Aβ_L change values between the two most recent longitudinal scans for each participant were then calculated, and Aβ(−) participants were classified as Aβ(−) accumulators if their change value exceeded either of the two cutoffs. The two most recent scans were chosen for this analysis since the majority of Aβ(−) individuals who eventually turned out to be accumulators were on non-accumulating trajectories prior to the most recent scan. Thus, evaluating the Aβ_L change value between the two most recent scans provides a better representation of Aβ_L change in the actual Aβ accumulation phase of Aβ(−) accumulators than if several points during the non-accumulating phase were included as well. For both cutoff methods, Aβ(−) accumulators displayed Aβ_L change values distinguishable from Aβ(−) non-accumulators. Additionally, no significant difference was observed between the Aβ_L change values of the Aβ(−) accumulator, Aβ-converter and Aβ(+) groups. This finding suggests that Aβ(−) accumulators follow a similar trajectory of Aβ_L change to that of Aβ(+) individuals, highlighting the usefulness of longitudinal imaging for detecting the very earliest stages of Aβ progression in DS detected with PET amyloid imaging. Given the Aβ(−) accumulators and the Aβ-converter/Aβ(+) group, estimated sample sizes necessary to detect a 25% reduction in annual Aβ change with 80% power (alpha 0.01) were determined. The estimated sample size was smallest in the Aβ-converter/Aβ(+) group (59), followed by larger sample size for the Aβ(−) accumulators (79). This analysis was repeated for an alpha of 0.05, in which the sample sizes for the Aβ-converter/Aβ(+) and Aβ(−) accumulator groups reduced to 39 and 53, respectively, suggesting that relatively small sample sizes would be needed to monitor treatment effects in both early and late intervention studies.

While Aβ(+) status is used to confirm the presence of AD-related pathology when cognitive impairments have been observed, an understanding of how subthreshold Aβ accumulation

can predict future AD-related cognitive decline is less understood. Some longitudinal studies have attempted to relate cognitive change with subthreshold Aβ accumulation in non-DS populations measured with SUVr but found no observable relation (Jack et al., 2009; Villemagne et al., 2013), likely due to small sample sizes and short follow-up periods. However, a larger study with longer durations between baseline and follow-up scans revealed subtle associations between subthreshold Aβ SUVr and cognitive change (Landau et al., 2018). The authors of that study note that removal of participants with fewer than three time points improved the statistical significance of the associations, suggesting the change calculated from participants with only two time points were primarily influenced by SUVr variability (Landau et al., 2018). Another longitudinal study in late-onset AD found that individuals with subthreshold Aβ accumulation demonstrated tau increase that correlated with worsening cognitive performance, emphasizing the importance of longitudinal imaging to better characterize early Aβ change (Hanseeuw et al., 2019). Furthermore, Leal et al. (2018) reports that very low levels of Aβ predicted neocortical tau spread over a 5 year period with a temporal lag between accumulation of these biomarkers and observable cognitive decline (Leal et al., 2018). In the current study, we highlight the capability of measuring subthreshold Aβ change with longitudinal imaging to better characterize the earliest stages within the natural history of Aβ progression in DS. All of the DS participants in the current study that were classified as Aβ(−) accumulators underwent at least three time points of image collection spanning five to eight years following the baseline visit, suggesting that longitudinal imaging studies will require several follow-up visits over a fairly long duration in order to capture both the Aβ(−) and Aβ accumulation phases necessary to accurately characterize early Aβ accumulation. Our analysis of Aβ_L change revealed that Aβ accumulation at subthreshold detection levels (i.e., prior to being Aβ(+)) is comparable to that observed for individuals who are Aβ(+), suggesting that longitudinal imaging can help lead to the underlying factors causing early accumulation.

A recent study evaluating longitudinal cognitive change in DS identified cognitive decline up to 20 years prior to the typical age of dementia diagnosis (~55 years), suggesting that the optimal recruitment age for clinical trials falls between 36 and 45 years (Hithersay et al., 2020). With the mean age of Aβ(+) in our cohort of ~46 years and the identification of subthreshold Aβ accumulators through longitudinal imaging, our findings suggest that the current cutoff for Aβ(+) of 20.0 Aβ_L may be too conservative to identify the earliest Aβ accumulators for clinical trial recruitment. Therefore, knowledge of these early Aβ accumulators in DS through longitudinal imaging was used to inform a more sensitive Aβ(+) cutoff to identify the beginning of Aβ detection using a single PET scan. With the Aβ_L change cutoffs of C_K and C_{2SD} as reference, a range of potential Aβ(+) cutoffs (i.e. 10–25 Aβ_L with increments of 0.1 Aβ_L) were explored. The Aβ_L value that maximized both the Youden's J Index (YI) and overall percentage agreement (OPA) with C_K or C_{2SD} was selected as the most optimal Aβ(+) cutoff for early Aβ deposition. The most optimal Aβ(+) cutoff was 13.0 Aβ_L using C_K as reference, and 13.3 Aβ_L using C_{2SD} as reference. The cutoff of 13.3 Aβ_L showed slightly higher YI and OPA with the Aβ_L change cutoff at identifying early Aβ accumulators when compared to the cutoff of 13.0 Aβ_L. Similar work has been performed in late-onset AD to identify subthreshold Aβ(+) cutoffs using Centiloids as the outcome measure to match both changes in cognition and increases in longitudinal Aβ

slopes (Farrell et al., 2020). The authors report several cutoffs in the range of 15.0–18.5 Centiloids that accurately identify early Aβ retention (Farrell et al., 2020). Another study derived a PET cutoff of 12 Centiloids in late-onset AD to match a previously established cerebrospinal fluid Aβ_{42} cutoff for Aβ(+), suggesting that fluid biomarkers can be used in conjunction with PET amyloid imaging to better define the earliest stages of Aβ accumulation (Salvadó et al., 2019). To match our findings in DS to the cutoffs determined in late-onset AD, Centiloid values were calculated in our DS cohort following previously described methodology (Klunk et al., 2015), and the Aβ_{L} values were then linearly transformed into units of Centiloids. The value of 13.3 Aβ_{L} corresponds to 18.0 Centiloids, falling within the range of optimal Aβ(+) cutoffs for determining early Aβ change in late-onset AD.

Due to the substantial number of participants that completed only two PiB scans to date, the current study was limited to analysis based on Aβ change between the baseline and most recent scans. As more scans are obtained for these participants, future work in this population will involve longitudinal modeling to better characterize the earliest stages of Aβ accumulation. Additionally, future studies will explore the relationship between Aβ accumulation and neuropsychological measures of cognition to match Aβ change with cognitive decline in DS. Another limitation to the current study involved classifying Aβ(−) accumulators using cutoffs derived from the same sample. This framework of Aβ(−) accumulator classification and the new Aβ(+) cutoff for early Aβ retention should be validated by applying them prospectively to new cases or by applying them to the non-DS population in future longitudinal studies. Additionally, longitudinal imaging in DS should be used in conjunction with plasma or cerebrospinal fluid measures of Aβ to better predict membership in an Aβ(−) accumulator group given a single PET scan.

Conclusion

Using the Aβ_{L} metric, modeled PiB images generated at different stages of AD progression present a method of visualizing regional longitudinal Aβ change in DS. Longitudinal Aβ_{L} trajectories were capable of distinguishing Aβ accumulators from non-accumulators in DS, and Aβ_{L} change was strongly associated with age, with the mean age at Aβ(+) conversion of ~ 46 years. Similar to late-onset AD, the annual rate of global Aβ change in DS was ~ 3 Aβ_{L}/year. Longitudinal imaging allowed for identification of subthreshold Aβ accumulation during the earliest stages of AD progression in which Aβ(−) accumulators with DS revealed similar rates of Aβ change to those that were Aβ(+), suggesting that longitudinal imaging can inform the identification of very early Aβ accumulators for clinical intervention studies. Using knowledge of these early Aβ accumulators, a new Aβ(+) cutoff of 13.3 Aβ_{L} was derived to better identify early Aβ retention given a single PET scan.

Acknowledgements

ABC-DS: The Alzheimer’s Biomarkers Consortium - Down Syndrome (ABC-DS) project is a longitudinal study of cognition and blood based, genetic and imaging biomarkers of Alzheimer’s Disease. This study is funded by the National Institute on Aging (NIA) grants [U01AG051406, R01AG031110, U54HD090256] and the National Institute for Child Health and Human Development (NICHD). We thank the ABC-DS study participants and the ABC-DS research and support staff for their contributions to this study.

This manuscript has been reviewed by ABC-DS investigators for scientific content and consistency of data interpretation with previous ABC-DS study publications. We acknowledge the ABC-DS study participants and the ABC-DS research and support staff for their contributions to this study. The content is solely the responsibility of the authors and does not necessarily represent the official views of the NIH.

References

Annus T, Wilson LR, Hong YT, Acosta-Cabronero J, Fryer TD, Cardenas-Blanco A, Smith R, Boros I, Coles JP, Aigbirhio FI, Menon DK, Zaman SH, Nestor PJ, Holland AJ, 2016. The pattern of amyloid accumulation in the brains of adults with Down syndrome. Alzheimer's Dement. 12, 538–545. doi: 10.1016/j.jalz.2015.07.490. [PubMed: 26362596]

Bateman RJ, Xiong C, Benzinger TLS, Fagan AM, Goate A, Fox NC, Marcus DS, Cairns NJ, Xie X, Blazey TM, Holtzman DM, Santacruz A, Buckles V, Oliver A, Moulder K, Aisen PS, Ghetti B, Klunk WE, McDade E, Martins RN, Masters CL, Mayeux R, Ringman JM, Rossor MN, Schofield PR, Sperling RA, Salloway S, Morris JC, 2012. Clinical and biomarker changes in dominantly inherited Alzheimer's disease. N. Engl. J. Med 367, 795–804. doi: 10.1056/NEJ-Moa1202753. [PubMed: 22784036]

Cohen J, 1992. A power primer. Psychol. Bull 112, 155–159. doi: 10.1037/0033-2909.112.1.155. [PubMed: 19565683]

Cohen J, 1988. Statistical Power Analysis for the Behavioral Sciences, 2nd ed L. Erlbaum Associates, Hillsdale, N.J.

Cole JH, Annus T, Wilson LR, Remtulla R, Hong YT, Fryer TD, Acosta-Cabronero J, Cardenas-Blanco A, Smith R, Menon DK, Zaman SH, Nestor PJ, Holland AJ, 2017. Brain-predicted age in Down syndrome is associated with beta amyloid deposition and cognitive decline. Neurobiol. Aging 56, 41–49. doi: 10.1016/j.neurobiolaging.2017.04.006. [PubMed: 28482213]

Dunn LM, Dunn DM, 2007. Peabody Picture Vocabulary Test, 4th ed NCD Pearson, Inc., San Antonio, TX.

Farrell ME, Jiang S, Schultz AP, Properzi MJ, Price JC, Becker JA, Jacobs HIL, Hanseeuw BJ, Rentz DM, Villemagne VL, Papp KV, Mormino EC, Betensky RA, Johnson KA, Sperling RA, Buckley RF, 2020. Defining the lowest threshold for amyloid-PET to predict future cognitive decline and amyloid accumulation. Neurology doi: 10.1212/WNL.0000000000011214, 10.1212/WNL.0000000000011214.

Handen BL, Cohen AD, Channamalappa U, Bulova P, Cannon SA, Cohen WI, Mathis CA, Price JC, Klunk WE, 2012. Imaging brain amyloid in nondemented young adults with Down syndrome using Pittsburgh compound B. Alzheimer's Dement. 8, 496–501. doi: 10.1016/j.jalz.2011.09.229. [PubMed: 23102120]

Handen BL, Lott IT, Christian BT, Schupf N, OBryant S, Mapstone M, Fagan AM, Lee JH, Tudorascu D, Wang M-C, Head E, Klunk W, Ances B, Lai F, Zaman S, Krinsky-McHale S, Brickman AM, Rosas HD, Cohen A, Andrews H, Hartley S, Silverman W The Alzheimer's Biomarker Consortium-Down Syndrome (ABC-DS), 2020. The Alzheimer's biomarker consortium-Down syndrome: rationale and methodology. Alzheimer's Dement.: Diagn. Assess. Dis. Monit 12, e12065. doi: 10.1002/dad2.12065.

Hanseeuw BJ, Betensky RA, Jacobs HIL, Schultz AP, Sepulcre J, Becker JA, Cosio DMO, Farrell M, Quiroz YT, Mormino EC, Buckley RF, Papp KV, Amariglio RA, Dewachter I, Ivanoiu A, Huijbers W, Hedden T, Marshall GA, Chhatwal JP, Rentz DM, Sperling RA, Johnson K, 2019. Association of amyloid and Tau with cognition in preclinical Alzheimer disease: a longitudinal study. JAMA Neurol. 76, 915. doi: 10.1001/jamaneurol.2019.1424.

Hartley SL, Handen BL, Devenny DA, Hardison R, Mihaila I, Price JC, Cohen AD, Klunk WE, Mailick MR, Johnson SC, Christian BT, 2014. Cognitive functioning in relation to brain amyloid-β in healthy adults with Down syndrome. Brain 137, 2556–2563. doi: 10.1093/brain/awu173. [PubMed: 24993958]

Hithersay R, Baksh RA, Startin CM, Wijeratne P, Hamburg S, Carter B, Strydom A, 2020. Optimal Age and Outcome Measures for Alzheimer's disease Prevention Trials in People With Down syndrome. Alzheimer's & Dementia n/a doi: 10.1002/alz.12222.

Jack CR, Lowe VJ, Weigand SD, Wiste HJ, Senjem ML, Knopman DS, Shiung MM, Gunter JL, Boeve BF, Kemp BJ, Weiner M, Petersen RC, 2009. Serial PIB and MRI in normal, mild cognitive impairment and Alzheimer's disease: implications for sequence of pathological events in Alzheimer's disease. Brain 132, 1355–1365. doi: 10.1093/brain/awp062. [PubMed: 19339253]

Jack CR, Wiste HJ, Lesnick TG, Weigand SD, Knopman DS, Vemuri P, Pankratz VS, Senjem ML, Gunter JL, Mielke MM, Lowe VJ, Boeve BF, Petersen RC, 2013. Brain β-amyloid load approaches a plateau. Neurology 80, 890–896. doi: 10.1212/WNL.0b013e3182840bbe. [PubMed: 23446680]

Jennings D, Seibyl J, Sabbagh M, Lai F, Hopkins W, Bullich S, Gimenez M, Reininger C, Putz B, Stephens A, Catafau AM, Marek K, 2015. Age dependence of brain β-amyloid deposition in Down syndrome. Neurology 84, 500. doi: 10.1212/WNL.0000000000001212. [PubMed: 25568295]

Klunk WE, Engler H, Nordberg A, Wang Y, Blomqvist G, Holt DP, Bergström M, Savitcheva I, Huang G-F, Estrada S, Ausén B, Debnath ML, Barletta J, Price JC, Sandell J, Lopresti BJ, Wall A, Koivisto P, Antoni G, Mathis CA, Långström B, 2004. Imaging brain amyloid in Alzheimer's disease with Pittsburgh compound-B. Ann. Neurol 55, 306–319. doi: 10.1002/ana.20009. [PubMed: 14991808]

Klunk WE, Koeppe RA, Price JC, Benzinger TL, Devous MD, Jagust WJ, Johnson KA, Mathis CA, Minhas D, Pontecorvo MJ, Rowe CC, Skovronsky DM, Mintun MA, 2015. The Centiloid project: standardizing quantitative amyloid plaque estimation by PET. Alzheimer's Dement. 11, 1–15. doi: 10.1016/j.jalz.2014.07.003,.e4. [PubMed: 25443857]

Klunk WE, Price JC, Mathis CA, Tsopelas ND, Lopresti BJ, Ziolko SK, Bi W, Hoge JA, Cohen AD, Ikonomovic MD, Saxton JA, Snitz BE, Pollen DA, Moonis M, Lippa CF, Swearer JM, Johnson KA, Rentz DM, Fischman AJ, Aizenstein HJ, DeKosky ST, 2007. Amyloid deposition begins in the striatum of presenilin-1 mutation carriers from two unrelated pedigrees. J. Neurosci 27, 6174–6184. doi: 10.1523/JNEUROSCI.0730-07.2007. [PubMed: 17553989]

Knopman DS, Lundt ES, Therneau TM, Albertson SM, Gunter JL, Senjem ML, Schwarz CG, Mielke MM, Machulda MM, Boeve BF, Jones DT, Graff-Radford J, Vemuri P, Kantarci K, Lowe VJ, Petersen RC, Jack CR, Alzheimer's Disease Neuroimaging Initiative, 2020. Association of initial β-amyloid levels with subsequent flortaucipir positron emission tomography changes in persons without cognitive impairment. JAMA Neurol. doi: 10.1001/jamaneurol.2020.3921.

Landau SM, Fero A, Baker SL, Koeppe R, Mintun M, Chen K, Reiman EM, Jagust WJ, 2015. Measurement of longitudinal β-amyloid change with 18F-florbetapir PET and standardized uptake value ratios. J. Nucl. Med 56, 567–574. doi: 10.2967/jnumed.114.148981. [PubMed: 25745095]

Landau SM, Horng A, Jagust WJ, 2018. Memory decline accompanies subthreshold amyloid accumulation. Neurology 90, e1452–e1460. doi: 10.1212/WNL.0000000000005354. [PubMed: 29572282]

Landt J, D'Abrera JC, Holland AJ, Aigbirhio FI, Fryer TD, Canales R, Hong YT, Menon DK, Baron J-C, Zaman SH, 2011. Using positron emission tomography and carbon 11–labeled Pittsburgh compound B to image brain fibrillar β-amyloid in adults with Down syndrome: safety, acceptability, and feasibility. Arch. Neurol 68, 890–896. doi: 10.1001/archneurol.2011.36. [PubMed: 21403005]

Lao PJ, Betthauser TJ, Hillmer AT, Price JC, Klunk WE, Mihaila I, Higgins AT, Bulova PD, Hartley SL, Hardison R, Tumuluru RV, Murali D, Mathis CA, Cohen AD, Barnhart TE, Devenny DA, Mailick MR, Johnson SC, Handen BL, Christian BT, 2016. The effects of normal aging on amyloid-β deposition in nondemented adults with Down syndrome as imaged by carbon 11–labeled Pittsburgh compound B. Alzheimer's Dement. 12, 380–390. doi: 10.1016/j.jalz.2015.05.013. [PubMed: 26079411]

Lao PJ, Handen BL, Betthauser TJ, Cody KA, Cohen AD, Tudorascu DL, Stone CK, Price JC, Johnson SC, Klunk WE, Christian BT, 2018. Imaging neurodegeneration in Down syndrome: brain templates for amyloid burden and tissue segmentation. Brain Imaging Behav. doi: 10.1007/s11682-018-9888-y.

Lao PJ, Handen BL, Betthauser TJ, Mihaila I, Hartley SL, Cohen AD, Tudorascu DL, Bulova PD, Lopresti BJ, Tumuluru RV, Murali D, Mathis CA, Barnhart TE, Stone CK, Price JC, Devenny DA, Mailick MR, Klunk WE, Johnson SC, Christian BT, 2017. Longitudinal changes in amyloid

positron emission tomography and volumetric magnetic resonance imaging in the nondemented Down syndrome population. Alzheimer's Dement.: Diagn. Assess. Dis. Monit 9, 1–9. doi: 10.1016/j.dadm.2017.05.001.

Leal SL, Lockhart SN, Maass A, Bell RK, Jagust WJ, 2018. Subthreshold amyloid predicts Tau deposition in aging. J. Neurosci 38, 4482–4489. doi: 10.1523/JNEU-ROSCI.0485-18.2018. [PubMed: 29686045]

Lopresti BJ, Klunk WE, Mathis CA, Hoge JA, Ziolko SK, Lu X, Meltzer CC, Schimmel K, Tsopelas ND, DeKosky ST, Price JC, 2005. Simplified quantification of Pittsburgh compound B amyloid imaging PET studies: a comparative analysis. J. Nucl. Med 46, 1959–1972. [PubMed: 16330558]

Mak E, Bickerton A, Padilla C, Walpert MJ, Annus T, Wilson LR, Hong YT, Fryer TD, Coles JP, Aigbirhio FI, Christian BT, Handen BL, Klunk WE, Menon DK, Nestor PJ, Zaman SH, Holland AJ, 2019. Longitudinal trajectories of amyloid deposition, cortical thickness, and tau in Down syndrome: a deep-phenotyping case report. Alzheimer's Dement.: Diagn. Assess. Dis. Monit 11, 654–658. doi: 10.1016/j.dadm.2019.04.006.

Matthews DC, Lukic AS, Andrews RD, Marendic B, Brewer J, Rissman RA, Mosconi L, Strother SC, Wernick MN, Mobley WC, Ness S, Schmidt ME, Rafii MS, 2016. Dissociation of Down syndrome and Alzheimer's disease effects with imaging. Alzheimer's Dement.: Transl. Res. Clin. Intervent 2, 69–81. doi: 10.1016/j.trci.2016.02.004.

McCarron M, McCallion P, Reilly E, Dunne P, Carroll R, Mulryan N, 2017. A prospective 20-year longitudinal follow-up of dementia in persons with Down syndrome. J. Intellect. Disabil. Res 61, 843–852. doi: 10.1111/jir.12390. [PubMed: 28664561]

McCarron M, McCallion P, Reilly E, Mulryan N, 2014. A prospective 14-year longitudinal follow-up of dementia in persons with Down syndrome. J. Intellect. Disabil. Res 58, 61–70. doi: 10.1111/jir.12074. [PubMed: 23902161]

Morris JC, Aisen PS, Bateman RJ, Benzinger TLS, Cairns NJ, Fagan AM, Ghetti B, Goate AM, Holtzman DM, Klunk WE, McDade E, Marcus DS, Martins RN, Masters CL, Mayeux R, Oliver A, Quaid K, Ringman JM, Rossor MN, Salloway S, Schofield PR, Selsor NJ, Sperling RA, Weiner MW, Xiong C, Moulder KL, Buckles VD, 2012. Developing an international network for Alzheimer research: the dominantly inherited Alzheimer network. Clin. Investig. (Lond.) 2, 975–984. doi: 10.4155/cli.12.93.

Oyama F, Cairns NJ, Shimada H, Oyama R, Titani K, Ihara Y, 1994. Down's syndrome: up-regulation of β-amyloid protein precursor and τ mRNAs and their defective coordination. J. Neurochem 62, 1062–1066. doi: 10.1046/j.1471-4159.1994.62031062.x. [PubMed: 8113792]

Rafii M, Wishnek H, Brewer J, Donohue M, Ness S, Mobley W, Aisen P, Rissman R, 2015. The down syndrome biomarker initiative (DSBI) pilot: proof of concept for deep phenotyping of Alzheimer's disease biomarkers in down syndrome. Front. Behav. Neurosci 9. doi: 10.3389/fnbeh.2015.00239.

Rafii MS, Lukic AS, Andrews RD, Brewer J, Rissman RA, Strother SC, Wernick MN, Pennington C, Mobley WC, Ness S, Matthews DC, 2017. PET imaging of Tau pathology and relationship to amyloid, longitudinal MRI, and cognitive change in down syndrome: results from the down syndrome biomarker initiative (DSBI). J. Alzheimer's Dis 60, 439–450. doi: 10.3233/JAD-170390. [PubMed: 28946567]

Rafii MS, Zaman S, Handen BL, 2020. Integrating biomarker outcomes into clinical trials for Alzheimer's disease in down syndrome. J. Prev. Alzheimers Dis doi: 10.14283/jpad.2020.35.

Remes AM, Laru L, Tuominen H, Aalto S, Kemppainen N, Mononen H, Någren K, Parkkola R, Rinne JO, 2008. Carbon 11–labeled Pittsburgh compound B positron emission tomographic amyloid imaging in patients with APP locus duplication. Arch. Neurol 65, 540–544. doi: 10.1001/archneur.65.4.540. [PubMed: 18413480]

Rumble B, Retallack R, Hilbich C, Simms G, Multhaup G, Martins R, Hockey A, Montgomery P, Beyreuther K, Masters CL, 1989. Amyloid A4 protein and its precursor in Down's syndrome and Alzheimer's disease. N. Engl. J. Med 320, 1446–1452. doi: 10.1056/NEJM198906013202203. [PubMed: 2566117]

Sabbagh MN, Chen K, Rogers J, Fleisher AS, Liebsack C, Bandy D, Belden C, Protas H, Thiyyagura P, Liu X, Roontiva A, Luo J, Jacobson S, Malek-Ahmadi M, Powell J, Reiman EM, 2015. Florbetapir PET, FDG PET, and MRI in Down syndrome individuals with and without

Alzheimer's dementia. Alzheimer's Dement. 11, 994–1004. doi: 10.1016/j.jalz.2015.01.006. [PubMed: 25849033]

Salvadó G, Molinuevo JL, Brugulat-Serrat A, Falcon C, Grau-Rivera O, Suárez-Calvet M, Pavia J, Niñerola-Baizán A, Perissinotti A, Lomeña F, Minguillon C, Fauria K, Zetterberg H, Blennow K, Gispert JD, Camí J, Cacciaglia R, Crous-Bou M, Deulofeu C, Dominguez R, Gotsens X, Gramunt N, Hernandez L, Huesa G, Huguet J, León M, Marne P, Menchón T, Milà M, Operto G, Pascual M, Polo A, Pradas S, Sala-Vila A, Sánchez-Benavides G, Segundo S, Soteras A, Tenas L, Vilanova M, Vilor-Tejedor NFor the Alzheimer's Disease Neuroimaging Initiative, for the A.S., 2019. Centiloid cut-off values for optimal agreement between PET and CSF core AD biomarkers. Alzheimer's Res. Ther 11, 27. doi: 10.1186/s13195-019-0478-z. [PubMed: 30902090]

Schupf N, 2002. Genetic and host factors for dementia in Down's syndrome. Br. J. Psychiatry 180, 405–410. doi: 10.1192/bjp.180.5.405. [PubMed: 11983636]

Sinai A, Mokrysz C, Bernal J, Bohnen I, Bonell S, Courtenay K, Dodd K, Gazizova D, Hassiotis A, Hillier R, McBrien J, McCarthy J, Mukherji K, Naeem A, Perez-Achiaga N, Rantell K, Sharma V, Thomas D, Walker Z, Whitham S, Strydom A, 2018. Predictors of age of diagnosis and survival of Alzheimer's disease in down syndrome. J. Alzheimer's Dis 61, 717–728. doi: 10.3233/JAD-170624. [PubMed: 29226868]

Tryputsen V, DiBernardo A, Samtani M, Novak GP, Narayan VA, Raghavan N Initiative, the A.D.N., 2015. Optimizing regions-of-interest composites for capturing treatment effects on brain amyloid in clinical trials. J. Alzheimer's Dis 43, 809–821. doi: 10.3233/JAD-131979. [PubMed: 25114074]

Tudorascu DL, Anderson SJ, Minhas DS, Yu Z, Comer D, Lao P, Hartley S, Laymon CM, Snitz BE, Lopresti BJ, Johnson S, Price JC, Mathis CA, Aizenstein HJ, Klunk WE, Handen BL, Christian BT, Cohen AD, 2019. Comparison of longitudinal Aβ in nondemented elderly and Down syndrome. Neurobiol. Aging 73, 171–176. doi: 10.1016/j.neurobiolaging.2018.09.030. [PubMed: 30359879]

Villemagne VL, Ataka S, Mizuno T, Brooks WS, Wada Y, Kondo M, Jones G, Watanabe Y, Mulligan R, Nakagawa M, Miki T, Shimada H, O'Keefe GJ, Masters CL, Mori H, Rowe CC, 2009. High striatal amyloid β-peptide deposition across different autosomal Alzheimer disease mutation types. Arch. Neurol 66, 1537–1544. doi: 10.1001/archneurol.2009.285. [PubMed: 20008660]

Villemagne VL, Burnham S, Bourgeat P, Brown B, Ellis KA, Salvado O, Szoeke C, Macaulay SL, Martins R, Maruff P, Ames D, Rowe CC, Masters CL, 2013. Amyloid β deposition, neurodegeneration, and cognitive decline in sporadic Alzheimer's disease: a prospective cohort study. Lancet Neurol. 12, 357–367. doi: 10.1016/S1474-4422(13)70044-9. [PubMed: 23477989]

Whittington A, Gunn RN, 2018. Amyloid Load – a more sensitive biomarker for amyloid imaging. J. Nucl. Med doi: 10.2967/jnumed.118.210518, jnumed.118.210518.

Whittington A, Sharp DJ, Gunn RN, 2018. Spatiotemporal distribution of β-amyloid in Alzheimer disease is the result of heterogeneous regional carrying capacities. J. Nucl. Med 59, 822–827. doi: 10.2967/jnumed.117.194720. [PubMed: 29146694]

Youden WJ, 1950. Index for rating diagnostic tests. Cancer 3, 32–35. doi: 10.1002/1097-0142(1950)3:1<32::AID-CNCR2820030106>3.0.CO;2-3. [PubMed: 15405679]

Zammit MD, Laymon CM, Betthauser TJ, Cody KA, Tudorascu DL, Minhas DS, Sabbagh MN, Johnson SC, Zaman SH, Mathis CA, Klunk WE, Handen BL, Cohen AD, Christian BT, 2020. Amyloid accumulation in Down syndrome measured with amyloid load. Alzheimer's Dement.: Diagn. Assess. Dis. Monit 12, e12020. doi: 10.1002/dad2.12020.

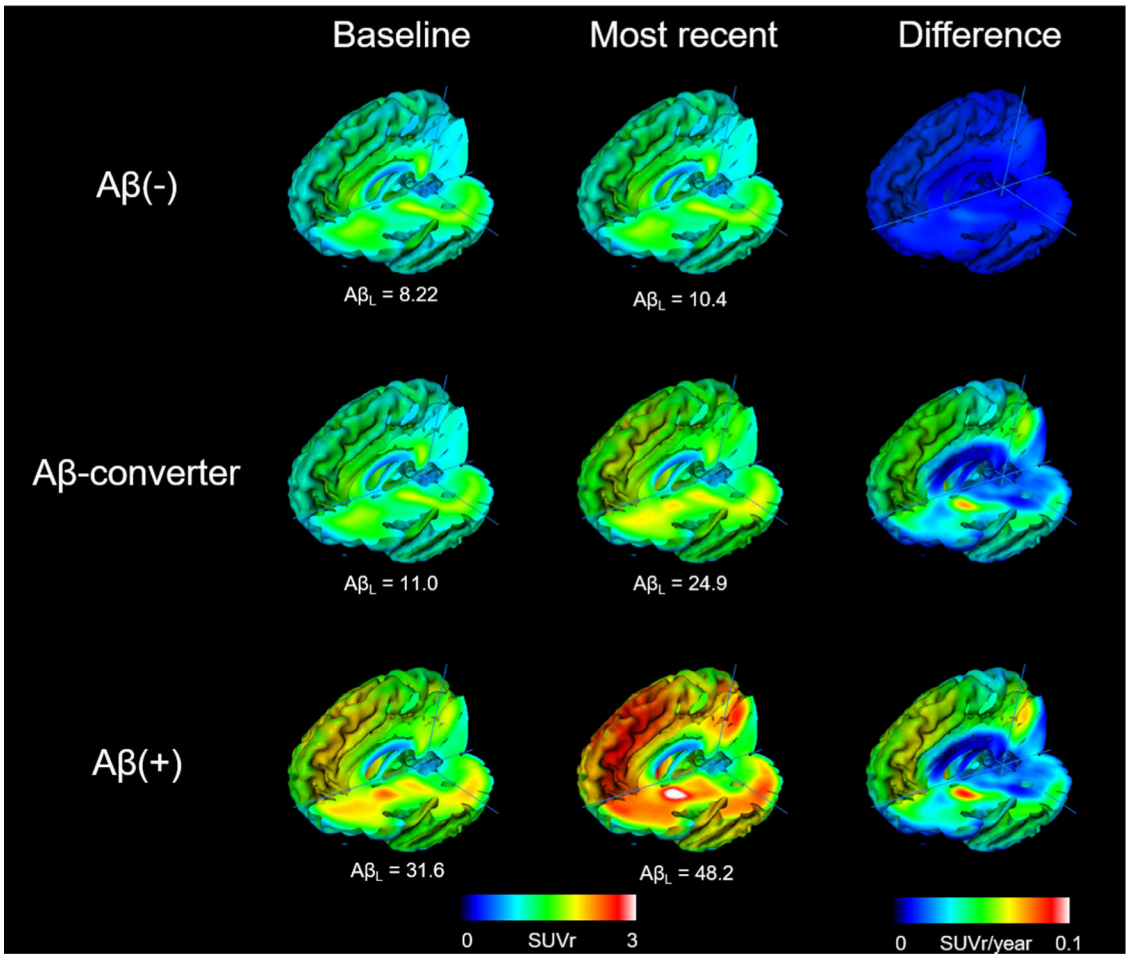

Fig. 1.

Modeled PiB SUVr and SUVr difference images (units of SUVr/year) for the Aβ(−), Aβ-converter and Aβ(+) groups generated from Eq. (1). SUVr images are overlaid with an MRI surface projection from a healthy DS brain (no Aβ and no MCI/AD consensus).

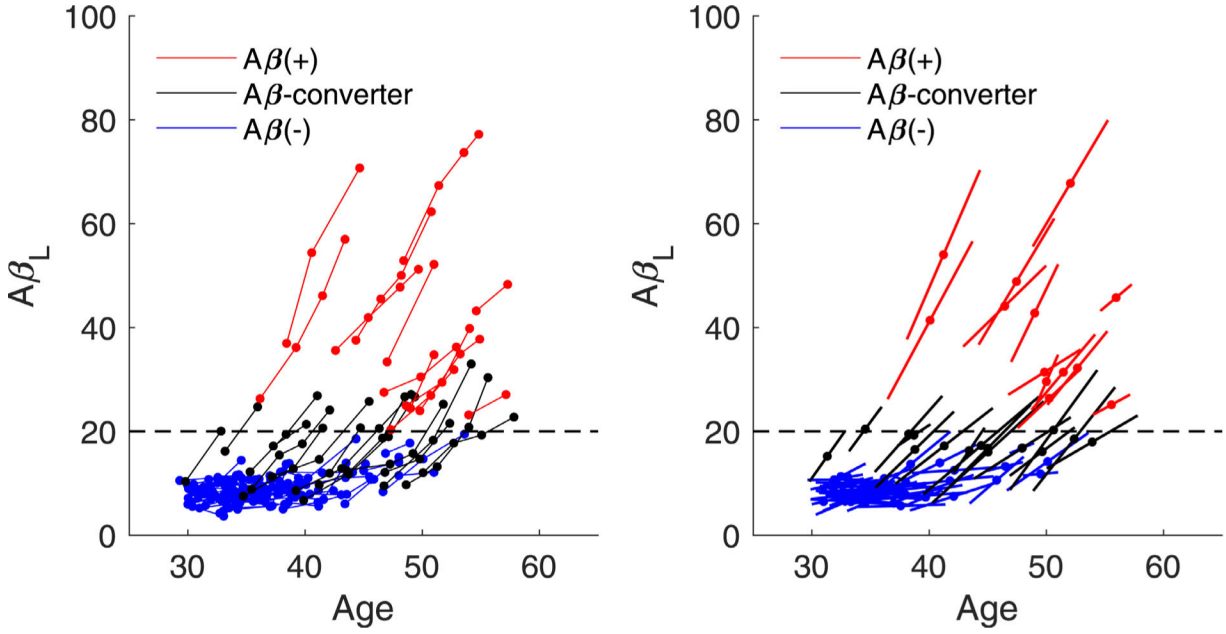

Fig. 2.

Longitudinal Aβ_L with respect to age for Aβ(−), Aβ-converter and Aβ(+) groups (left). Longitudinal Aβ_L with respect to age displayed as linear trajectories centered on the mean age and mean Aβ_L for each participant (right).

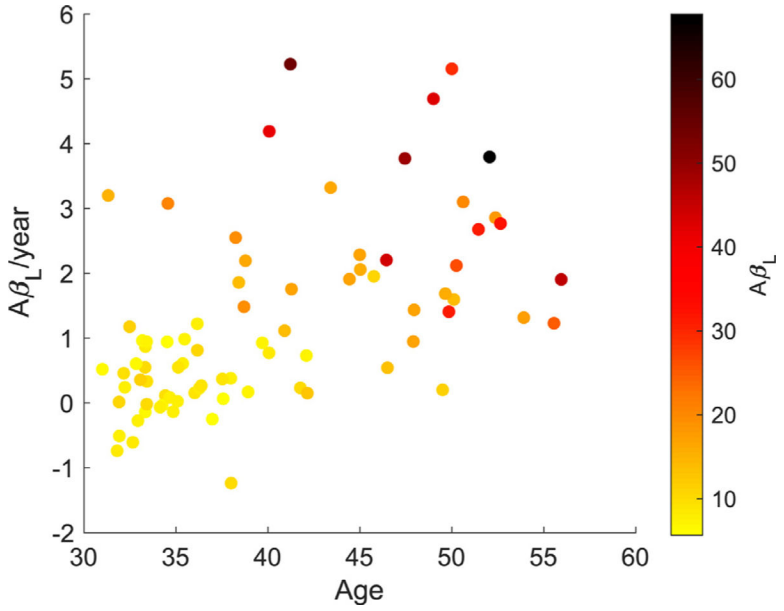

Fig. 3.

Positive association between Aβ_L change values (Aβ_L/year) and age for each participant with Down syndrome.

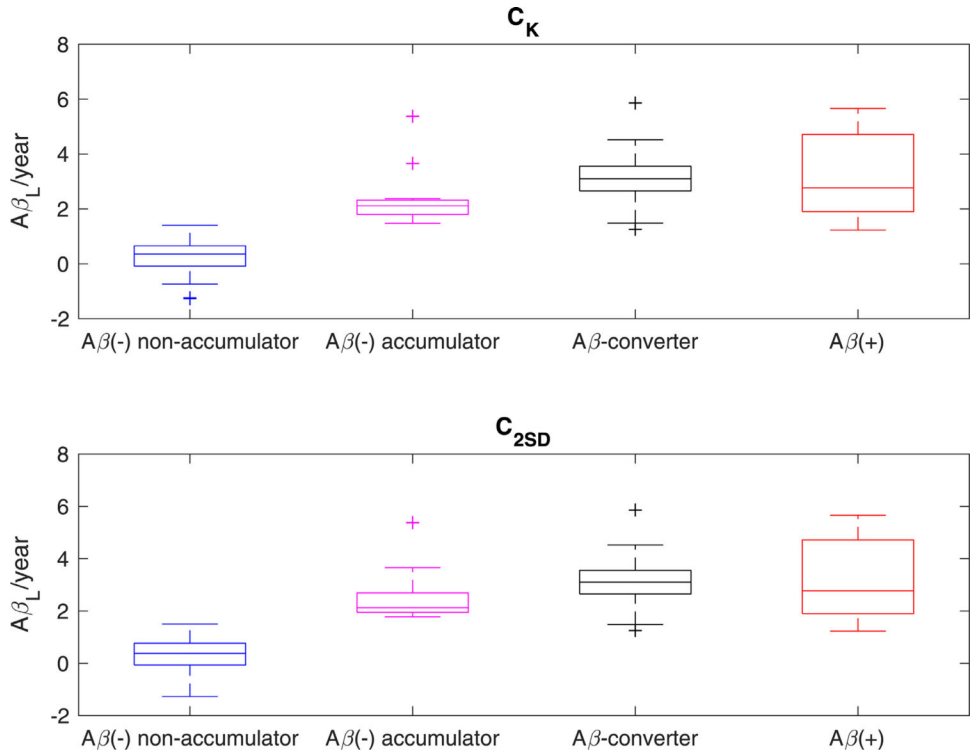

Fig. 4.

Aβ_L change values (Aβ_L/year) between the two most recent longitudinal time points for Aβ(−) non-accumulator, Aβ(−) accumulator, Aβ-converter and Aβ(+) groups categorized by the Aβ_L change cutoffs using the k-means clustering (C_K; top) and mean + 2*SD methods (C_{2SD}; bottom).

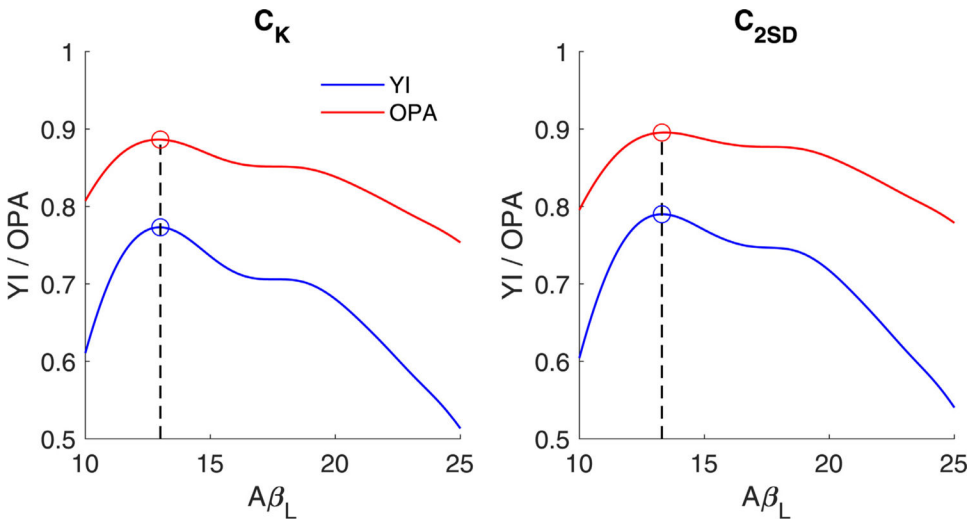

Fig. 5.

Youden's J Index (YI) and overall percentage agreement (OPA) response curves with respect to Aβ_L using the cutoffs C_K (left) and C_{2SD} (right) as reference. The Aβ_L value with maximum YI and OPA was selected as the optimal cutoff for subthreshold Aβ(+).

Table 1

Down syndrome participant demographics categorized by the number of longitudinal PiB scans performed.

	All	***N* = 2 PiB scans**	***N* = 3 PiB scans**	***N* = 4 PiB scans**
Number of participants	**79**	24	30	25
Sex (M/F)	**39/40**	9/15	16/14	14/11
Chronological age (years)	**42.7 (7.28)**	40.9 (7.89)	41.9 (7.30)	45.2 (5.77)
PPVT mental age (years)	**7.61 (3.19)**	7.31 (2.35)	7.47 (3.75)	8.11 (3.13)
Time between scans (mean (SD) years)	**2.64 (0.71)**	2.80 (0.49)	2.66 (0.84)	2.57 (0.66)
Aβ(−)	**50**	16	20	14
Aβ-converter	**16**	4	5	7
Aβ(+)	**13**	4	5	4
MC1-DS/AD consensus	**12**	1	5	6
APOE ε4 carriers	**13**	5	5	3

Table 2

Regional SUVr differences (SUVr/year) from the modeled SUVr images for each Aβ group.

Region	Aβ(−)	Aβ-converter	Aβ(+)
Anterior cingulate	0.010	0.043	0.063
Frontal	0.008	0.038	0.056
Parietal	0.010	0.047	0.069
Precuneus	0.010	0.052	0.077
Striatum	0.012	0.060	0.088
Temporal	0.006	0.030	0.044